

Negative refractive index due to chirality

Jiangfeng Zhou,¹ Jianfeng Dong,^{2,1} Bingnan Wang,¹ Thomas Koschny,^{1,3} Maria Kafesaki,³ and Costas M. Soukoulis^{1,3}

¹*Ames Laboratory and Department of Physics and Astronomy, Iowa State University, Ames, Iowa 50011, USA*

²*Institute of Optical Fiber Commun. and Network Tech., Ningbo University, Ningbo 315211, China*

³*Institute of Electronic Structure and Laser - Foundation for Research and Technology Hellas (FORTH), and Department of Materials Science and Technology, University of Crete, Greece*

We demonstrate experimentally and numerically that metamaterials based on bilayer cross wires give giant optical activity and circular dichroism and negative refractive index. The presented chiral design offers a much simpler geometry and more efficient way to realize negative refractive index at any frequency. We also developed a retrieval procedure for chiral materials which works successfully for circularly polarized waves.

PACS numbers: 78.20Ek, 41.20.Jb, 42.25.Ja

I. INTRODUCTION

Recently, chiral metamaterials were proposed as an alternative to realize negative refractive index¹⁻³. Chiral metamaterials are metamaterials made of unit cells without symmetry planes. It has been shown that backward waves exist in chiral media^{1,3}. A chiral material slab can focus the incident EM beams and can be used as a perfect lens^{4,5}. In 2004, the canonical helix³ and the twisted Swiss-rolle metal structures² for microwave applications have been discussed as possible candidates to achieve negative refractive index. Later on, the bilayer rosette shaped chiral metamaterial was proposed and fabricated at microwave frequency^{6,7} and at optical regime⁸⁻¹⁰. It exhibited a very strong rotary power in the microwave, near-infrared and visible spectral ranges. In the microwave spectral region, in terms of rotary power per wavelength, the bilayer structure rotates is five orders of magnitude stronger than a gyrotropic crystal of quartz⁶. It has been shown that the strong gyrotropy originates from the magnetic resonance of the bilayer metallic structure with anti-parallel current flowing in the bilayer metal wires¹¹. In this sense, the bilayer chiral structure is the chiral version of the short wire pair¹²⁻¹⁴ type of metamaterials. The planar chiral structure^{15,16} and chiral photonic crystal¹⁷ were proposed and fabricated. More recently, a chiral SRR consisting of double layers of SRRs was proposed to provide negative refractive index¹⁸.

In this letter we demonstrate experimentally and numerically the negative refraction using the bilayer cross-wire design. We show that the negative refraction originate from the 3D chiral properties of the bilayer cross wires. Unlike the conventional negative index material designs, such as the split-ring resonator type design¹⁹ and fishnet designs²⁰, the chiral negative index material do not require simultaneously negative permittivity and permeability, and, therefore, the chiral design can offer much simpler geometry and a more efficient way to realize negative refraction index. Due to the asymmetric geometry of the cross-wire pairs, the cross coupling be-

tween the magnetic field and electric field happens at the chiral resonances and provide strong chirality around the resonance frequencies. Further study shows the chiral resonances are either electric resonance or magnetic resonance of the short wire pairs. The negative refractive index of chiral metamaterial arise from this strong chirality, which split the refractive indices, n_{\pm} , of the two circularly polarized waves and make the refractive index of one circularly polarization become negative². Our study show that two resonance modes exist for the cross-wire pairs. The resonance mode at lower frequency is a magnetic resonance mode with anti-parallel currents, while the resonance mode at higher frequency is an electric resonance with parallel currents.

We develop a retrieval procedure adopting uniaxial bi-anisotropic model to calculate the effective parameters, μ , ϵ , κ and n_{\pm} , of the chiral metamaterial design. We prove that the existence of the negative index originating from the chirality, κ of the cross-wire metamaterial. As a comparison, non-chiral version of cross-wires pair design does not show any negative refractive index. Finally, we study the current distribution for both the electric and the magnetic resonances, and find out that the electric and the magnetic resonances are the symmetric and antisymmetric resonance modes of the coupled short wire resonances, respectively. From this point of view, the bilayer cross-wire structures can be considered as the chiral version of short-wire pairs, which have been designed as magnetic resonator providing negative permittivity, μ , at microwave and optical frequencies¹²⁻¹⁴.

II. MODEL

The layout of the proposed structure is shown in Fig. 1. A 18×14 array cross-wires is patterned on a double side copper-clad FR-4 board. The overall size of our sample is $279 \times 216 \text{ mm}^2$. The dielectric constant of the FR-4 board is $\epsilon_r = 4.5 + 0.15i$. The transmission coefficient is measured by a HP 8364B network analyzer with two Narda standard horn antennas. Since the eigen solutions of the elec-

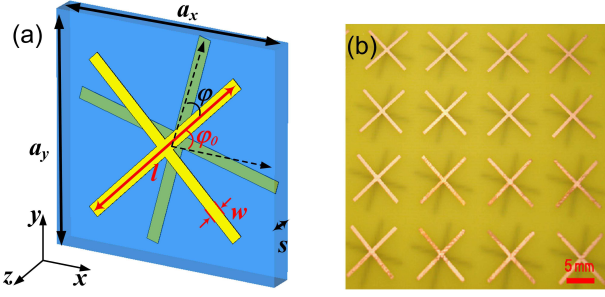


FIG. 1: (a) Schematic representation of one unit cell of the cross-wire structure. (b) Photograph of one side of a fabricated microwave-scale cross-wire sample. The geometry parameters are given by $a_x = a_y = 15\text{mm}$, $l = 14\text{ mm}$, $w = 1\text{ mm}$, $s = 1.6\text{ mm}$, $\phi_0 = 45^\circ$, $\phi = 30^\circ$.

tromagnetic (EM) wave in chiral materials are two circularly polarized EM waves, i.e. the right-handed circularly polarized wave (RCP,+) and the left-handed circularly polarized wave (LCP,-), correspondingly, four transmission coefficients, T_{++} , T_{-+} , T_{+-} and T_{--} , should be obtained to fully characterize the response of the chiral metamaterials. In our experiments, four linear transmission coefficients, T_{xx} , T_{yx} , T_{xy} and T_{yy} , are measured and the circular transmission coefficients, T_{++} , T_{-+} , T_{+-} and T_{--} are converted from the linear transmission coefficients using the following equation,

$$\begin{pmatrix} T_{++} & T_{+-} \\ T_{-+} & T_{--} \end{pmatrix} = \frac{1}{2} \times \begin{pmatrix} (T_{xx} + T_{yy}) + i(T_{xy} - T_{yx}) & (T_{xx} - T_{yy}) - i(T_{xy} + T_{yx}) \\ (T_{xx} - T_{yy}) + i(T_{xy} + T_{yx}) & (T_{xx} + T_{yy}) - i(T_{xy} - T_{yx}) \end{pmatrix} \quad (1)$$

Fig. 2(a) and (b) show the simulated and measured transmission coefficients, T_{++} and T_{--} , as a function of frequency, respectively (the cross coupling transmission, T_{-+} and T_{+-} , are negligible, which are not shown here). Due to the asymmetric geometry along the propagating direction, the transmission responses for RCP and LCP split into two curves. Notice two resonance peaks are observed at frequencies, $f = 6.3$ and 7.4 GHz, in both T_{++} and T_{--} curves. For the first resonance at 6.3 GHz, the transmission dip for RCP, T_{++} , is much deeper than that for LCP, T_{--} , which implies the resonance for RCP is much stronger than LCP. While, for the second resonance at 7.4 GHz, we observe the resonance for LCP is much stronger than RCP. Use the standard definition²¹ of the for polarization azimuth rotation, $\theta = [\arg(T_{++}) - \arg(T_{--})]/2$, and the ellipticity, $\eta = \arcsin\left(\frac{|T_{++}| - |T_{--}|}{|T_{++}| + |T_{--}|}\right)$, of elliptically polarized light, we calculated the polarization changes of an linearly polarized wave incident on the cross wire structures. The simulated and measured azimuth rotation, θ , and ellipticity, η , are presented in Fig. 2(c),(e) and (d),(f), respectively. At the resonance frequencies of 6.3 GHz and 7.3 GHz, the azimuth rotation and ellipticity reach their

maximum values, $(\theta = -89^\circ, \eta = -28^\circ)$ and $(\theta = -130^\circ, \eta = -28^\circ)$, respectively. In the region between two resonance peaks (around 6.9 GHz), which is the region with low loss and nearly zero dichroism, we observe rotation of polarization of -40° with $\eta \approx 0$.

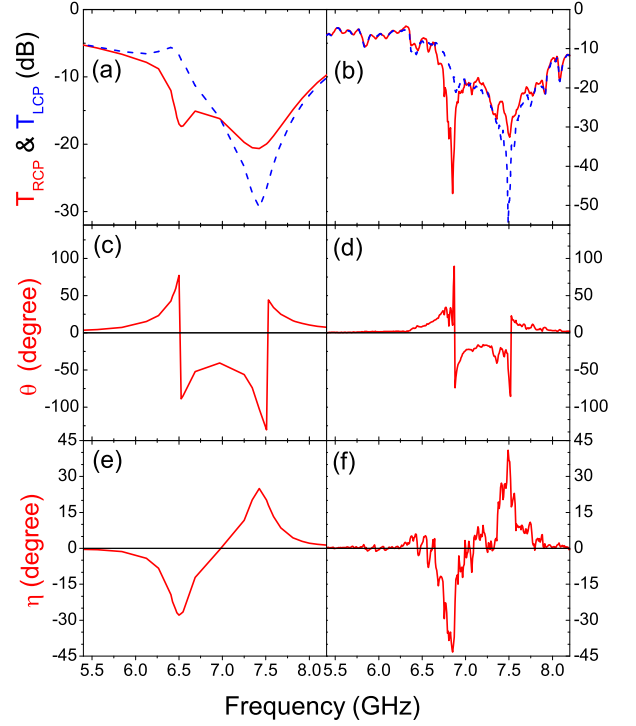


FIG. 2: (a) and (b): Simulated and measured transmission coefficient for the right circularly polarized (red solid) and the left circularly polarized (blue dashed) electromagnetic wave, respectively. (c) and (d): Simulated and measured rotary power, θ , respectively. (e) and (f): Simulated and measured ellipticity angle, η , respectively.

III. RETRIEVAL PROCEDURE

In order to study the effective parameters of chiral metamaterial, we develop a retrieval procedure based on an uniaxial bi-anisotropic model. The cross wire pairs design can be modeled as a reciprocal uniaxial bi-anisotropic medium and the constitutive equation is given by

$$\begin{pmatrix} \mathbf{D} \\ \mathbf{B} \end{pmatrix} = \begin{pmatrix} \epsilon_0 \epsilon & -i\kappa/c_0 \\ i\kappa/c_0 & \mu_0 \mu \end{pmatrix} \begin{pmatrix} \mathbf{E} \\ \mathbf{H} \end{pmatrix}, \quad (2)$$

where ϵ_0 , μ_0 , and c_0 are the permittivity, permeability, and the speed of light in vacuum, respectively. Assuming $\exp(-i\omega t)$ time dependent, the eigen solution of electromagnetic wave in bi-isotropic media is circular polarized plane waves, and the polarization is either left-handed circular polarized (LCP) or right handed polarized (RCP). The refractive indices for LCP and RCP are

given by^{22,23}

$$n_{\pm} = \sqrt{\epsilon\mu} \pm \kappa, \quad (3)$$

where (+) and (-) denote RCP and LCP. Both LCP and RCP have the same impedance given by $z/z_0 = \sqrt{\mu/\epsilon}$, where z_0 is the impedance of the vacuum.

From Eq. (3), one can immediately see that $n < 0$ for one of the polarizations if κ is large enough such that $\sqrt{\epsilon\mu} < \kappa$. It has been shown that the polarization azimuth rotation, θ , shows the rotary power is proportional to the chiral parameter, κ . Specifically, $\theta = \kappa k_0 d$, where k_0 and d are the wave vectors in a vacuum and the thickness of the bi-isotropic slab. Thus, the chiral materials with large rotary power, such as the bilayer structures and chiral SRRs, possibly possess the negative refractive index. However, it's not trivial to obtain negative refractive index by a chiral design with large azimuth rotation. One should keep in mind that the large value of azimuth angle, θ , happens at the resonances, where $\sqrt{\epsilon\mu}$ is also large, so κ should be large enough to overcome the large magnitude of $\sqrt{\epsilon\mu}$ to achieve negative n .

IV. RESULTS AND DISCUSSIONS

In Fig. 3, we present the refractive index for RCP and LCP, n_+ , n_- , the conventional definition of refraction index, $n = \sqrt{\epsilon\mu}$, and the chiral parameter, κ . Notice that n (black dotted curve) is positive through the whole frequency range from 5 to 9 GHz. However, n_+ (red solid) is negative from 6.5 to 7.0 GHz and n_- (blue dashed) has a negative region from 7.6 to 8.2 GHz. The chiral parameter (green dash-dotted curve) shows two resonances at 6.5 and 7.5 GHz, respectively. Above the first resonance frequency, κ is negative between 6.5 to 7 GHz, which leads to $n_{RCP} = \sqrt{\epsilon\mu} + \kappa < 0$ between 6.5 to 7.0 GHz. Similarly, Above the second resonance frequency, κ is positive and result in $n_{RCP} = \sqrt{\epsilon\mu} - \kappa < 0$ between 7.6 to 8.2 GHz. It is clear that the negative refractive index for RCP and LCP originate from the chiral parameter, κ . The observed negative refractive index $n_{RCP} = -2.5$ at 6.8 GHz has the figure of merit $FOM = |\text{Re}(n)/\text{Im}(n)| = 0.75$ and $n_{LCP} = -1$ at 7.8 GHz has $FOM = 0.5$. The figure of merit is relatively low compared to the conventional negative index material designs such as SRRs or fishnet. The low FOM is due to the high loss of this chiral metamaterial design. Further study shows the loss mainly originate from the lossy dielectric spacer. If low loss dielectric materials is used in the cross wire design, the FOM can be improve substantially. For instance, in our numerical simulations, we obtained $FOM \approx 10$ using dielectric spacer with $\epsilon_r = 4.5 + 0.005i$.

Fig. 4 shows the n_+ , n_- , n and κ for a non-chiral cross-wire pairs with the twisted angle $\phi = 0$, (as shown in Fig. 1). Since the geometry is symmetric with respect to the EM wave propagating direction, we do not expect any difference between RCP and LCP, and, therefore, no negative refractive index. As shown in Fig. 4,

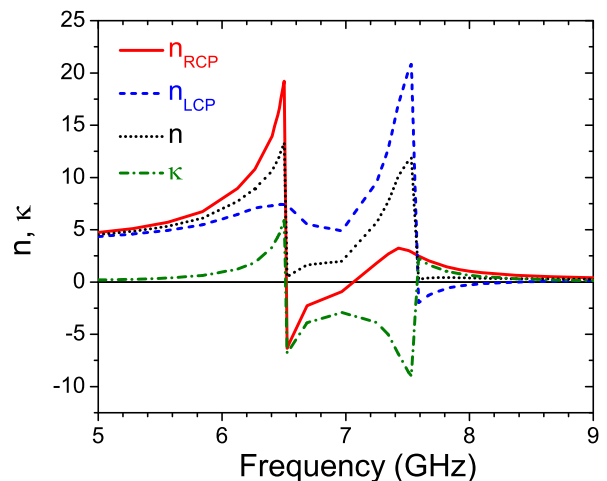


FIG. 3: The retrieved effective refractive index for the right circularly polarized EM wave, n_+ (red solid), and the left circularly polarized EM wave, n_- (blue dashed). The black dotted curve shows the refractive index calculated by the permittivity and the permeability, $n = \sqrt{\epsilon\mu}$, and the green dash-dotted curve shows the chiral parameter, κ . All of the effective parameters are calculated from the simulation data.

n_+ (red solid) and n_- (blue dashed) are exactly identical, moreover, they are both same as n (black dotted). Although two resonances are observed again, unlike the chiral cross-wires pairs, no negative index exists around the resonance frequencies. The chiral parameter (green dash-dotted) is zero through the whole frequency range from 5 GHz to 9 GHz. Thus, we confirmed the negative refractive index observed in Fig. 3 is due to the chirality introduced by the asymmetry of the cross wire pairs.

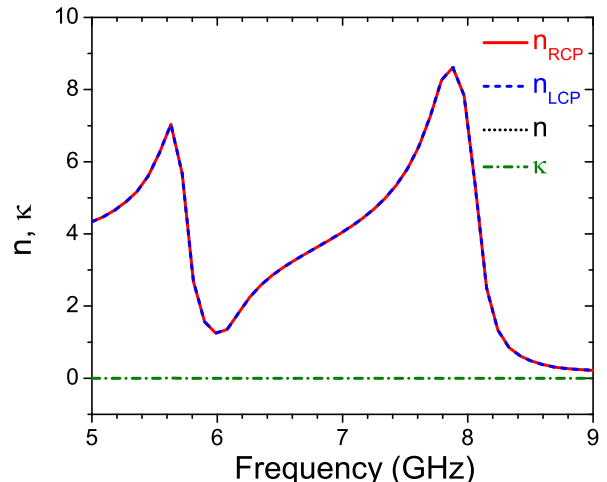


FIG. 4: The retrieved effective parameters, n_+ , n_- , n and κ , for a non-chiral cross-wire pairs. All of the geometry parameters are same as shown in Fig. 1 except $\phi = 0^\circ$.

In Fig. 5, we present the real parts of the permittivity, ϵ , and the permeability, μ , as a function of fre-

quency for the asymmetric cross wire pairs. Two resonances are observed in μ (blue dashed) at 6.5 GHz and ϵ (red solid) at 7.5 GHz, respectively. This demonstrate that the resonance observed in Fig. 2 and 3 at 6.5 GHz is a magnetic resonance and the resonance at 7.5 GHz is an electric resonance. The magnetic resonance gives the negative μ between 6.5 to 6.9 GHz, and the electric resonance give a negative ϵ between 7.6 to 9 GHz. There is no overlap region of negative ϵ and μ , therefore, $\text{Re}(n) = \text{Re}(\sqrt{\epsilon\mu}) > 0$, which is consistent with the observation of $\text{Re}(n) > 0$ shown in Fig. 3.

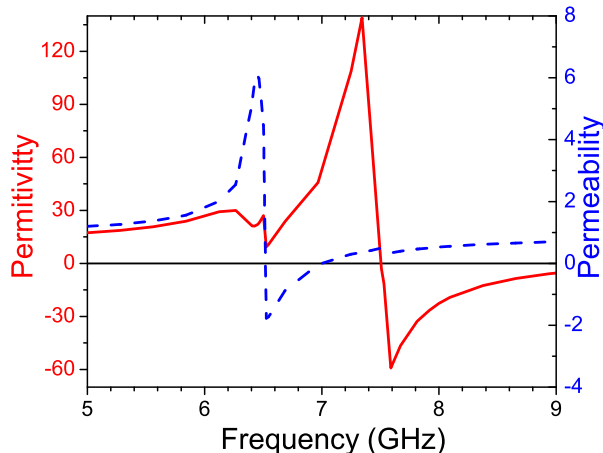


FIG. 5: The real part of the effective permittivity (red solid) and the effective permeability (blue dashed), extracted from the simulation data.

In order to understand the mechanism of the resonances for the cross-wire pair design, we studied the current density distribution as shown in Fig. 6. Notice that, at the magnetic resonance, the anti-parallel current exists on the top and bottom layer of cross wire pairs (Fig. 6(a)), which is an asymmetric resonance modes. In Fig. 6(b), one can see parallel current flowing on the two layers of wires, which is a symmetric resonance mode. The current distribution shows that the cross wire pairs can be viewed as a chiral version of the short wire pairs¹²⁻¹⁴, which has the similar current distributions in the symmetric and asymmetric resonance modes.

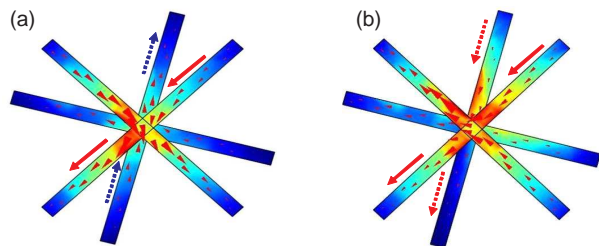


FIG. 6: The simulated current density distribution for the right circularly polarized EM wave at 6.5 GHz (a) and for the left circularly polarized EM wave at 7.5 GHz (b).

V. CONCLUSIONS

In summary, we have experimentally realized a bilayer cross wires with very adaptable properties including negative index of refraction due to chirality, giant optical activity and very large circular dichroism. We have performed numerical simulations that give evidence that the negative refractive index is due to the chiral nature of the metamaterial and not from the simultaneous negative ϵ and μ as for conventional negative index materials. In addition, we have developed a retrieval procedure that works well for chiral metamaterials. The geometry of the cross wire design is simple and easy-to-fabricate, and therefore, is more suitable for optical frequency applications compared to other type of bi-layer chiral metamaterial designs.

VI. ACKNOWLEDGMENTS

Work at Ames Laboratory was supported by the Department of Energy (Basic Energy Sciences) under contract No. DE-AC02-07CH11358. This work was partially supported by the Department of Navy, Office of the Naval Research (Award No. N00014-07-1-0359), European Community FET project PHOME (Contract No. 213390) and AFOSR under MURI grant (FA 9550-06-1-0337). The author Jianfeng Dong gratefully acknowledges support of the W.C. Wong Education Foundation, Hong Kong, the National Basic Research Program (973) of China (Grant No. 2004CB719805) and the National Natural Science Foundation of China (Grant No.60777037).

¹ S. Tretyakov, I. Nefedov, A. Sihvola, S. Maslovski, and C. Simovski, *J. Electromagnetic Waves Applications* **17**,

- ² J. B. Pendry, *Science* **306**, 1353 (2004),
- ³ S. Tretyakov, A. Sitivola, and L. Jylha, *Photonics Nanostructures-fundamentals Applications* **3**, 107 (2005).
- ⁴ Y. Jin and S. He, *Opt. Express* **13**, 4974 (2005).
- ⁵ C. Monzon and D. W. Forester, *Physical Review Letters* **95**, 123904 (pages 4) (2005).
- ⁶ A. V. Rogacheva, V. A. Fedotov, A. S. Schwanecke, and N. I. Zheludev, *Physical Review Letters* **97**, 177401 (pages 4) (2006).
- ⁷ E. Pulm, J. Zhou, J. Dong, V. A. Fedotov, T. Koschny, C. M. Soukoulis, and N. I. Zheludev, *Physical Review B* **Accepted** (2008).
- ⁸ E. Plum, V. A. Fedotov, A. S. Schwanecke, N. I. Zheludev, and Y. Chen, *Applied Physics Letters* **90**, 223113 (pages 3) (2007).
- ⁹ T. Vallius, K. Jefimovs, J. Turunen, P. Vahimaa, and Y. Svirko, *Applied Physics Letters* **83**, 234 (2003).
- ¹⁰ M. Decker, M. W. Klein, M. Wegener, and S. Linden, *Opt. Lett.* **32**, 856 (2007).
- ¹¹ Y. Svirko, N. Zheludev, and M. Osipov, *Applied Physics Letters* **78**, 498 (2001).
- ¹² V. M. Shalaev, W. S. Cai, U. K. Chettiar, H. K. Yuan, A. K. Sarychev, V. P. Drachev, and A. V. Kildishev, *Optics Letters* **30**, 3356 (2005).
- ¹³ J. F. Zhou, L. Zhang, G. Tuttle, T. Koschny, and C. M. Soukoulis, *Physical Review B (Condensed Matter and Materials Physics)* **73**, 041101 (pages 4) (2006).
- ¹⁴ G. Dolling, C. Enkrich, M. Wegener, J. F. Zhou, and C. M. Soukoulis, *Optics Letters* **30**, 3198 (2005).
- ¹⁵ V. A. Fedotov, P. L. Mladyonov, S. L. Prosvirnin, A. V. Rogacheva, Y. Chen, and N. I. Zheludev, *Physical Review Letters* **97**, 167401 (pages 4) (2006).
- ¹⁶ B. Bai, Y. Svirko, J. Turunen, and T. Vallius, *Physical Review A (Atomic, Molecular, and Optical Physics)* **76**, 023811 (pages 12) (2007).
- ¹⁷ M. Thiel, G. von Freymann, and M. Wegener, *Opt. Lett.* **32**, 2547 (2007).
- ¹⁸ L. Jelinek, R. Marqués, F. Mesa, and J. D. Baena, *Physical Review B (Condensed Matter and Materials Physics)* **77**, 205110 (pages 6) (2008).
- ¹⁹ D. Smith, W. Padilla, D. Vier, S. Nemat-Nasser, and S. Schultz, *Physical Review Letters* **84**, 4184 (2000).
- ²⁰ G. Dolling, C. Enkrich, M. Wegener, C. M. Soukoulis, and S. Linden, *Science* **312**, 892 (2006).
- ²¹ J. D. Jackson, *Classical Electrodynamics* (John Wiley, 1998), 3rd ed., ISBN 0-471-30932-X.
- ²² J. A. Kong, *Electromagnetic Wave Theory* (Cambridge, 2000).
- ²³ C. Monzon, *IEEE Trans. Antennas Propag.* **38**, 227 (1990).